

# Geophysical Research Letters<sup>®</sup>



## RESEARCH LETTER

10.1029/2022GL098286

# Sahel Rainfall Projections Constrained by Past Sensitivity to Global Warming

Jacob Schewe<sup>1</sup>  and Anders Levermann<sup>1,2,3</sup> 

<sup>1</sup>Potsdam Institute for Climate Impact Research, Potsdam, Germany, <sup>2</sup>Institute of Physics, Potsdam University, Potsdam, Germany, <sup>3</sup>Lamont-Doherty Earth Observatory, Columbia University, New York, NY, USA

### Key Points:

- We identify the response of Sahel rainfall to greenhouse gas-induced global warming in the historical record
- Many global climate models of the latest generation (Coupled Model Intercomparison Project Phase 6) do not reproduce the observed rainfall response
- Observational constraint reduces model spread and implies stronger rainfall increase under further warming than in full ensemble

### Supporting Information:

Supporting Information may be found in the online version of this article.

### Correspondence to:

J. Schewe,  
[schewe@pik-potsdam.de](mailto:schewe@pik-potsdam.de)

### Citation:

Schewe, J., & Levermann, A. (2022). Sahel rainfall projections constrained by past sensitivity to global warming. *Geophysical Research Letters*, 49, e2022GL098286. <https://doi.org/10.1029/2022GL098286>

Received 24 FEB 2022  
Accepted 12 SEP 2022

### Author Contributions:

**Conceptualization:** Jacob Schewe, Anders Levermann  
**Investigation:** Jacob Schewe  
**Methodology:** Jacob Schewe  
**Writing – original draft:** Jacob Schewe  
**Writing – review & editing:** Anders Levermann

**Abstract** Africa's central Sahel region has experienced prolonged drought conditions in the past, while rainfall has recovered more recently. Global climate models project anything from no change to a strong wetting trend under unabated climate change; and they have difficulty reproducing the complex historical record. Here we show that when a period of dominant aerosol forcing is excluded, a consistent wetting response to greenhouse-gas induced warming emerges in observed rainfall. Using the observed response coefficient estimate as a constraint, we find that Coupled Model Intercomparison Project Phase 6 climate models with a realistic past rainfall response show a smaller spread, and higher median, of projected future rainfall change, compared to the full ensemble. In particular, very small or negative rainfall trends are absent from the constrained ensemble. Our results provide further evidence for a robust Sahel rainfall increase in response to greenhouse-gas forcing, consistent with recent observations, and including the possibility of a very strong increase.

**Plain Language Summary** Rainfall is a critical resource for a large population in the African Sahel region, but rainfall levels have strongly varied in the past. It is unclear what will happen in the next decades, because some climate models suggest little to no change in average rainfall, while other models project a strong increase due to climate change. Our study aims to narrow down this uncertainty. In the past, both greenhouse gases and aerosols influenced Sahel rainfall, to different degrees during different periods; and models may not capture both mechanisms equally well. However, future rainfall changes will likely be driven mainly by greenhouse gas levels. We identify models that closely match the rainfall change that was observed in a recent period with dominant greenhouse gas forcing. These models also tend to project stronger rainfall increases than other models. Indeed, their multi-model mean projection is an increase by almost 50% by 2040; while none of them projects stable rainfall levels or even a reduction. Thus, it appears more likely now that rainfall in the Sahel will increase substantially over the next few decades.

## 1. Introduction

The Sahel region is home to a large and growing population (Guengant, 2017), to whom rainfall represents a critical resource for agriculture and other economic activities, but also a source of natural hazards such as flooding (Tschakert et al., 2010). On multidecadal timescales, the first half of the twentieth century has seen a rising trend in average Sahel rainfall, though frequently punctuated by anomalously dry years. This trend reversed in the second half of the century, and culminated in a prolonged period of drought conditions throughout the 1970s and 1980s that led to widespread famine and ecological deterioration. Since the 1990s, average rainfall has been rising again.

The importance and the variable history of Sahel rainfall prompt questions about its future evolution, which require an understanding of its drivers. Theoretical and modeling studies have shown that the long-term trends observed in the twentieth century were to a large extent a forced response to anthropogenic changes—greenhouse—gas and aerosol (precursor) emissions rather than an expression of internal variability of the climate system (Giannini et al., 2008). However, future projections from global climate models show considerable disagreement over the magnitude, and partly even the sign, of the expected response to future forcing scenarios (Giannini et al., 2008; Monerie et al., 2020; Schewe & Levermann, 2017). In this paper, we apply recent understanding of the causes of twentieth century rainfall trends in order to narrow the range of future rainfall projections in the latest generation of global climate models.

© 2022. The Authors.

This is an open access article under the terms of the [Creative Commons Attribution License](https://creativecommons.org/licenses/by/4.0/), which permits use, distribution and reproduction in any medium, provided the original work is properly cited.

A series of studies have shown that differences in sea surface temperature (SST) between the (sub-tropical) North Atlantic, and the tropical Atlantic or global oceans, can explain a large part of the observed Sahel rainfall variations on interannual and longer timescales (Biasutti et al., 2008; Giannini et al., 2013). These SST differences, in turn, are modulated by human-induced radiative forcings. Greenhouse-gas (GHG) emissions, which have been rising at a growing rate throughout the twentieth century, increase surface temperatures globally and persistently. On the other hand, scattering aerosols, mainly sulfate aerosols related to sulfur dioxide (SO<sub>2</sub>) emissions from the use fossil fuels, have a cooling effect on SST, which however is more localized and transient due to the shorter lifetime of tropospheric aerosols, compared to GHG.

The multi-decadal variations in Sahel rainfall have recently been attributed to the specific combination of these two forcings during the twentieth century (Giannini & Kaplan, 2019; Zhang et al., 2022). Specifically, the GHG-induced warming, in the tropics, increases atmospheric stability because surface warming is quickly disseminated vertically through deep convection, and then horizontally within the tropical upper atmosphere. This raises the energetic threshold for convection (Chou & Neelin, 2004). Rainfall at the margins of convective regions then depends on whether sufficient moisture gets imported at the lower level to meet this “upped ante.” It has been argued that the massive SO<sub>2</sub> emissions in the decades after World War II, in Europe and North America, and the resultant regional cooling effect of sulfate aerosols on North Atlantic SST, acted to limit moisture supply from the subtropical North Atlantic to the African monsoon (Giannini & Kaplan, 2019). When moisture import became increasingly insufficient to meet the rising convective threshold, this led to the observed decline in Sahel rainfall starting in the 1950s and accelerating in the 1960s. After aerosol precursor emissions in the North Atlantic sector declined in the 1980s and 1990s, subtropical North Atlantic SSTs rose in correspondence with the global GHG forcing, low-level atmospheric moisture content was able to catch up with the “upped ante,” and Sahel rainfall began to increase again.

This understanding implies that the response of Sahel rainfall to global warming is markedly different depending on whether or not GHG-induced warming is opposed by regional aerosol-induced cooling in the North Atlantic. Given that aerosol and aerosol precursor emissions in the North Atlantic sector are projected to remain low throughout the 21st century (Rao et al., 2017), it is the response to GHG-induced warming alone that will likely dominate the future evolution of Sahel rainfall. Thus, climate models which simulate that response accurately may also be suited for future projections, no matter whether or not they also capture the response to combined GHG and aerosol forcing well.

## 2. Data

We investigate the historical and SSP5-8.5 experiments from 39 models participating in the Coupled Model Intercomparison Project Phase 6 (CMIP6) (Eyring et al., 2016; O’Neill et al., 2016; Tebaldi et al., 2021). Where multiple realizations are available for a given model and experiment, we use the first one for our main analysis; in addition, we use multiple realizations for a subset of models to test the influence of internal variability. CMIP6 models and ensemble members are listed in Table S1 in Supporting Information S1. We focus on July–September average rainfall in the central Sahel region (0–30°E, 10–20°N), which is more susceptible to changes in remote moisture import than the coastal regions further to the West. Notably, the western Sahel is also more susceptible to slow changes in ocean circulation following atmospheric warming, and therefore shows a different long-term response to GHG emissions than the central Sahel (Monerie et al., 2021). To account for the possibility that models may get the monsoon dynamics qualitatively right but not the precise spatial distribution of rainfall anomalies, we also perform our analysis on rainfall averaged over model-specific, rectangular regions chosen to include the largest simulated rainfall anomaly, which are often somewhat offset from the common region denoted above. The corresponding figures are provided in Supporting Information.

Observational temperature and precipitation data are obtained from the University of East Anglia Climatic Research Unit (CRU) TS4.04 data set (Harris et al., 2020). Anthropogenic SO<sub>2</sub> emission data are obtained from the Community Emissions Data System (CEDS) (Hoesly et al., 2018); these data are also used as input for the CMIP6 historical experiments.

## 3. Results

Under the high GHG concentration scenario SSP5-8.5, most of the CMIP6 models project an increase in central Sahel rainfall in the course of the 21st century (Figure 1 and Figure S1 in Supporting Information S1). By the

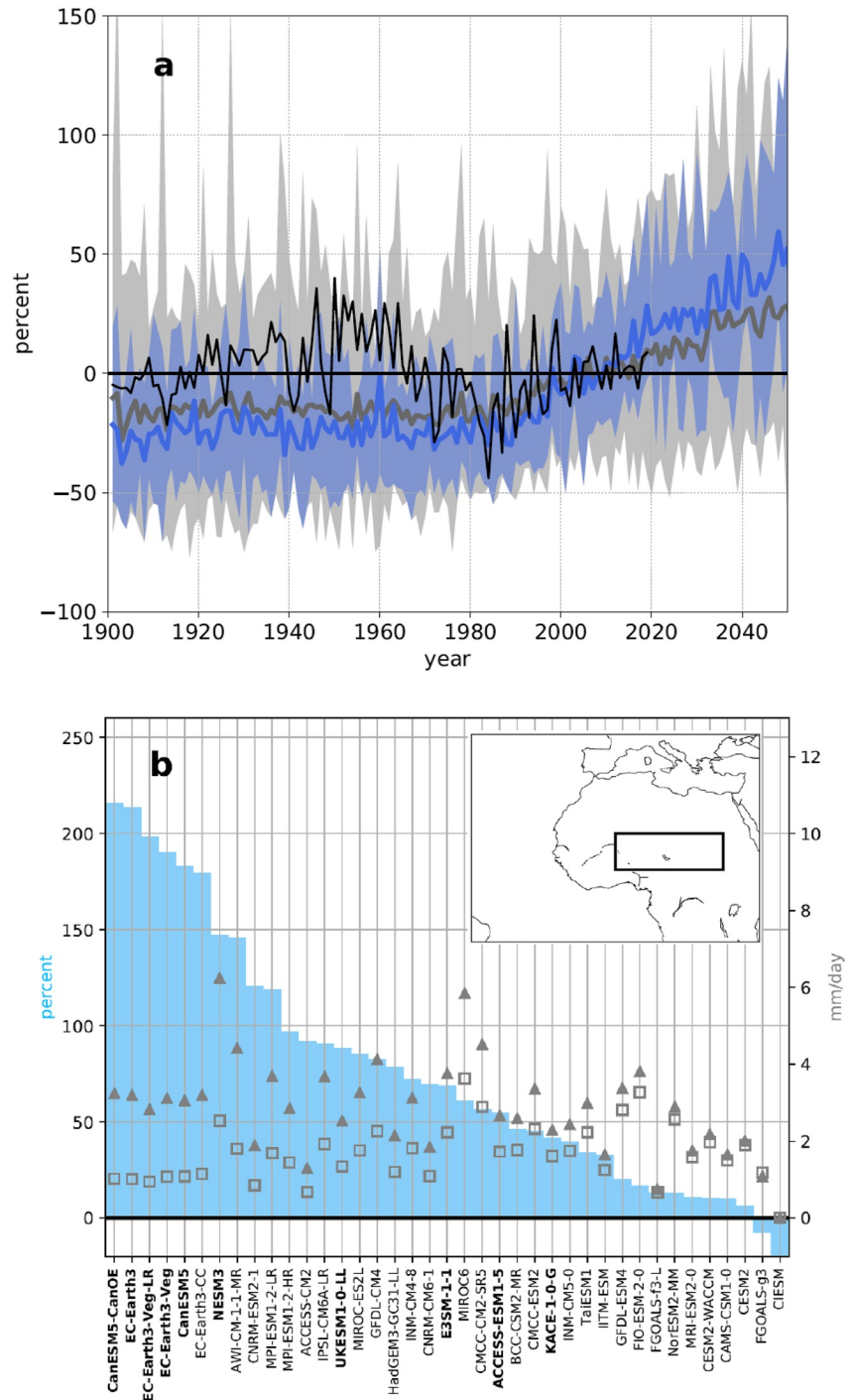


**Figure 1.** Sahel summer rainfall in Coupled Model Intercomparison Project Phase 6 coupled climate models under historical and SSP5-8.5 forcing. (a) Percentage deviation from the 1996 to 2019 average rainfall in the full ensemble (gray) and the constrained ensemble (blue), and in observations (CRU TS v4.04 (Harris et al., 2020); thin black line). Thick lines and shading show multi-model mean and envelope (minimum and maximum among models), respectively. (b) Percentage change in simulated average rainfall by the end of the 21st century (2071–2095) compared to the twentieth century average (1901–1999; bars, left vertical axis). Open squares and filled triangles show the simulated average rainfall during 1901–1999 and 2071–2095, respectively, in absolute terms (right vertical axis). The constrained ensemble is denoted by model names in bold font. Inset map indicates the central Sahel region studied. An extended version of panel (a) until 2,100 is provided in Figure S1 in Supporting Information S1.

2040s, the multi-model mean is about 25% above recent levels (Figure 1a, gray line); and comparing the end of the 21st century to the twentieth century average, the multi-model mean increase is around 70% (Figure S1 in Supporting Information S1). However, the spread across the model ensemble is large. Individual models project near-zero or even small negative changes in rainfall, while at the other extreme, some models show increases of around 200%, that is, a tripling of average rainfall amounts, between the twentieth century and the end of the 21st century (Figure 1b). The largest relative increases are found in the CanESM and EC-Earth 3 models, each of which have several variants in the ensemble, but which between each other are largely independent (Brunner et al., 2020), highlighting that models with very large rainfall increases cannot be treated as mere outliers.

Thus, the models in CMIP6 largely agree on the sign of the expected central Sahel rainfall change, and more so than in previous simulation rounds (Biasutti, 2013; Park et al., 2015); but given the broad and homogeneous distribution of projected rainfall changes across the CMIP6 ensemble, there remains a large uncertainty about the magnitude of this change. Constraining these centennial-scale projections with past observations is complicated by the earlier finding that mean biases in past Sahel rainfall simulations are a poor predictor of simulated future rainfall change (Monerie et al., 2017); and by the fact that the centennial-scale trend in the observations is very small. Indeed, average rainfall amounts in the early 21st century are roughly the same as during the early twentieth century (Figure 2a).

This is despite substantial decadal-scale trends in the data. In the first half of the twentieth century, central Sahel rainfall saw a rising trend, concurrent with the trend in global mean surface temperature. Beginning in the 1950s, however, rainfall gradually declined, leading into a period of devastating droughts in the 1970s and 1980s. Unlike with global mean temperature, which saw a relatively short period of moderate decline, the declining trend in Sahel rainfall did not reverse until about the late 1980s. It coincided with a period of steeply rising sulfate aerosol precursor emissions in Europe and North America, as well as globally, stemming from fossil fuel combustion (shading in Figure 2a).

Motivated by previous findings regarding Sahel rainfall response to GHG and aerosol forcing (Giannini & Kaplan, 2019), we divide the historical rainfall record into three parts: A period with steeply rising and, subsequently, high anthropogenic SO<sub>2</sub> emissions in the North Atlantic sector (AER, 1951–1995); as well as the periods before (PRE, 1901–1950) and after (POST, 1996–2019) this period. The PRE and POST periods correspond to rising trends in Sahel rainfall and a dominant role of GHG-induced surface warming as the forcing responsible for that trend; whereas the AER period corresponds to (mostly) declining Sahel rainfall and an important role of sulfate aerosols in inhibiting Atlantic moisture supply to the Sahel, as discussed above. We find, in both the PRE and POST periods, a very similar sensitivity of Sahel rainfall to global surface warming: About 0.7 mm/day per degree of warming (Figure 2b). This similarity suggests a coherent response of Sahel rainfall to surface warming in the absence of strong aerosol forcing.

Given that aerosol precursor emissions, at least in the OECD countries that are most relevant for North Atlantic aerosol pollution, are assumed to remain low (Lund et al., 2019; Rao et al., 2017), future Sahel rainfall changes should be dominated by GHG forcing as long as GHG concentrations keep increasing; which is the case in most SSP scenarios until the 2040s, and in SSP5-85 throughout the 21st century. Therefore, we use the response coefficient estimated from the POST period observations to constrain the model projections. We find that only ten of the 39 models fall within the 66% range of the estimated coefficient of 0.72; two more models fall just outside of it (Figure 3). About half of the models have a negative coefficient, that is, they show a decrease of Sahel rainfall with global warming during the POST period. Using the PRE period instead, we find similar results, although the models that fall within the 66% range of the observational estimate are not exactly the same (see Figure S2 in Supporting Information S1). We base our discussion in the main paper on the results from the POST period, since models might be more reasonably expected to reproduce this later period well given the stronger forcing and arguably better observational data compared to the PRE period.

The models' sensitivity of Sahel rainfall to warming in the recent past is correlated with the projected response to future warming, although the spread is large in particular among the models with a negative historical sensitivity (Figure 3). Especially at high warming, those models encompass the full spread of the ensemble, including models such as AWI-CM-1-1-MR, MIROC6, and MPI-ESM1-2-LR that show both a strongly negative response of rainfall to past warming, and a strong future rainfall increase. In contrast, the spread is smaller across those models that fall within the 66% range of the observed sensitivity during POST (histograms in Figure 3). In particular, none of these models projects less than a 0.5 mm/day increase of average rainfall under SSP5-8.5. Most project an increase of 0.6–1.2 mm/day at 2°C global warming, and of 1–2 mm/day at 3.5°C warming; while

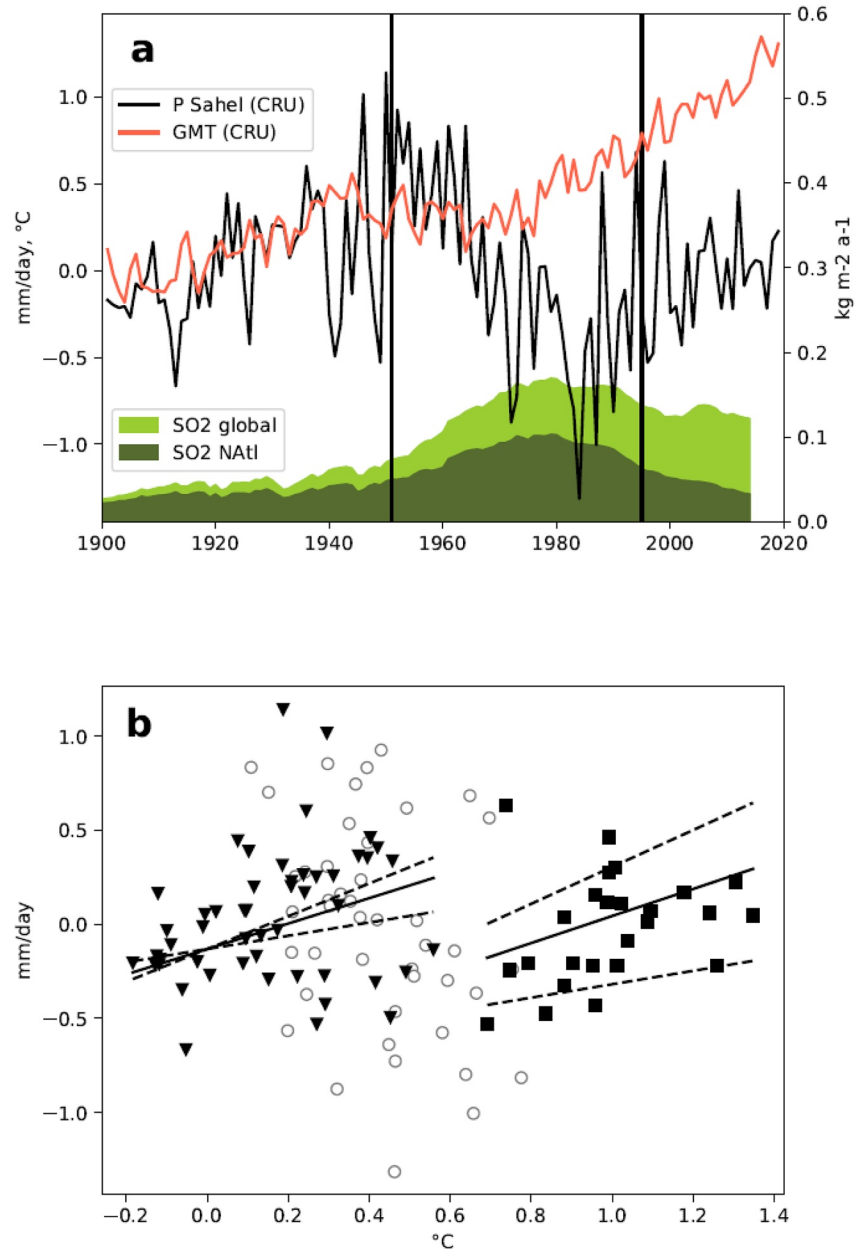


**Figure 2.** (a) Observed anomalies in global annual mean temperature (GMT, red) and Sahel summer rainfall (averaged over 0–30°E, 10–20°N and July–September; black), from CRU TS v4.04 (Harris et al., 2020). GMT anomalies are measured against the 1986–2005 average, and displayed relative to pre-industrial (1765–1850) conditions using an estimated warming of 0.75°C from pre-industrial up to 1986–2005 (Hawkins et al., 2017). Precipitation anomalies are relative to the twentieth century average (1901–1999). Dark and light green shading shows total anthropogenic sulfur dioxide (SO<sub>2</sub>) emissions in the North Atlantic sector (100°W–50°E, 0–90°N) and globally, respectively (Hoesly et al., 2018). (b) Sahel rainfall and GMT anomalies from (a), plotted against each other. The data is divided into a period with high SO<sub>2</sub> emissions in the North Atlantic sector (1951–1995, gray circles), as well as before (PRE; triangles) and after (POST; squares) this period; as indicated by the vertical lines in (a). Solid lines show Theil-Sen slopes fitted separately to the PRE and POST data, and dashed lines indicate the 66% compatibility intervals of the slope estimates. The central estimate of the slope—the sensitivity of Sahel precipitation to global warming—is 0.68 for PRE and 0.72 for POST.

one of the models with the strongest agreement with observed sensitivity, NESM3, projects an increase of 3 mm/day at 3.5°C warming. Correspondingly, the median rainfall change of the constrained ensemble is substantially higher than that of the full ensemble: About 0.85 compared to 0.65 mm/day at 2°C, and 1.4 compared to 1.0 mm/day at 3.5°C.

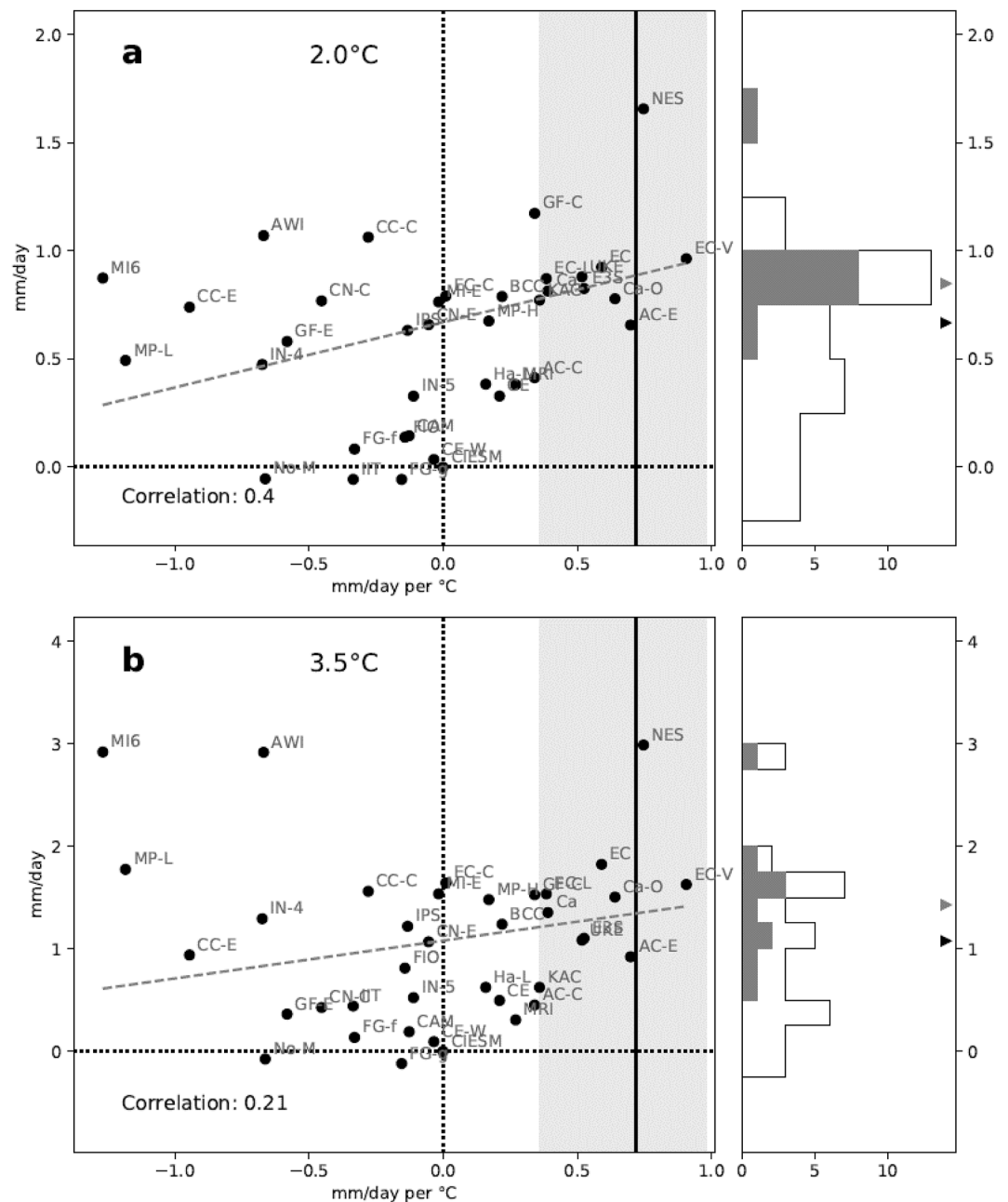


**Figure 3.** Coupled Model Intercomparison Project Phase 6 (CMIP6) Sahel (0–30°E, 10–20°N) rainfall projections at (a) 2.0°C and (b) 3.5°C global warming, constrained with past sensitivity to Greenhouse-gas-induced warming. Left panels show simulated change in Sahel rainfall versus simulated historical precipitation sensitivity. Each symbol represents a CMIP6 model (see Table S1 in Supporting Information S1). Solid vertical line is the precipitation sensitivity calculated from observations (slopes in Figure 2b), for the POST period. Shaded area indicates the corresponding 66% compatibility interval. Precipitation sensitivity was calculated analogously for the models. Dashed gray lines show Theil-Sen slopes. Precipitation at 0°C, 2.0°C, and 3.5°C global warming is calculated as the median of all values within a bin of 0.5°C width centered around the respective warming level, and the difference between the two levels is shown on the y-axis. Right panels show histograms of rainfall change in the full ensemble (black outline) and the ensemble of models whose precipitation sensitivity falls within the observed range (gray bars). The corresponding ensemble median is given by the black and gray triangle, respectively.

In terms of relative changes within the next two decades, the multi-model mean of the constrained ensemble projects a rainfall increase by nearly 50% by the 2040s, compared to about 25% in the full ensemble (Figure 1, blue line). This difference grows to almost 100% (constrained ensemble) versus about 50% (full ensemble) by the end of the century; all relative to recent rainfall levels (Supporting Information Figure 1). Analysis of monthly

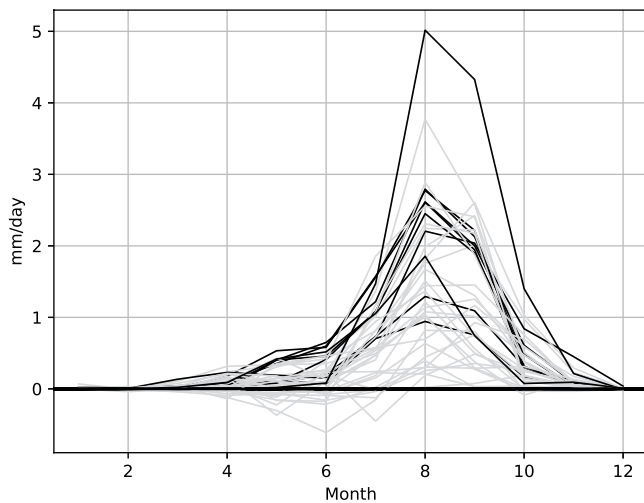


**Figure 4.** Change (future minus past) in monthly average Sahel (0–30°E, 10–20°N) daily precipitation between the end of the twentieth century (1970–1999) and the end of the 21st century (2070–2099). Models with historical precipitation sensitivity within the 66% range of observations (cf. Figure 3) are shown in black, others in gray.

rainfall changes shows that while some CMIP6 models project a substantial drying in the beginning of the rainy season, this is not observed in the constrained ensemble: All models whose sensitivity to historical warming is close to the observed one, also show an increase of rainfall throughout the rainy season in the future (Figure 4). This is consistent with the idea of an intensifying West African monsoon system in a warming atmosphere with increasing moisture supply from oceanic evaporation.

Next, we explore to what extent these differences between models can be traced to differences in SST simulations. Observations show that during each of the PRE, AER, and POST periods, SSTs have warmed in the tropical Atlantic (Figure 5). However, outside the tropics in the North Atlantic, patterns are distinctly different between the periods: Pronounced (and stronger than in the tropics) warming during PRE and POST, but little warming and, north of the subtropics, even cooling, during AER. This is consistent with the strong regional influence of aerosols during AER discussed above. Both the PRE and POST warming as well as the AER cooling signal are centered in the northwestern Atlantic.

Models, on the other hand, show a variety of SST change patterns (Figure S6 and S7 in Supporting Information S1). Especially for the POST period, those models whose precipitation sensitivity is broadly in line with the one estimated from observations, also tend to agree with the observed SST

change patterns; while those with a very different (often negative) sensitivity often also show SST change patterns that are very different from observations (Figure S7, and Table S2 in Supporting Information S1). Many of the latter models show SST cooling, instead of warming, in the northern North Atlantic during POST. This suggests that the ability of models to reproduce at least the correct sign of the sensitivity of Sahel rainfall to GHG-induced global warming might be linked to their ability to simulate a realistic response of North Atlantic SST to such warming. Nevertheless, there is large variety and complexity in SST change patterns, and a number of models simulate realistic SST change patterns but negative precipitation sensitivity or vice versa.

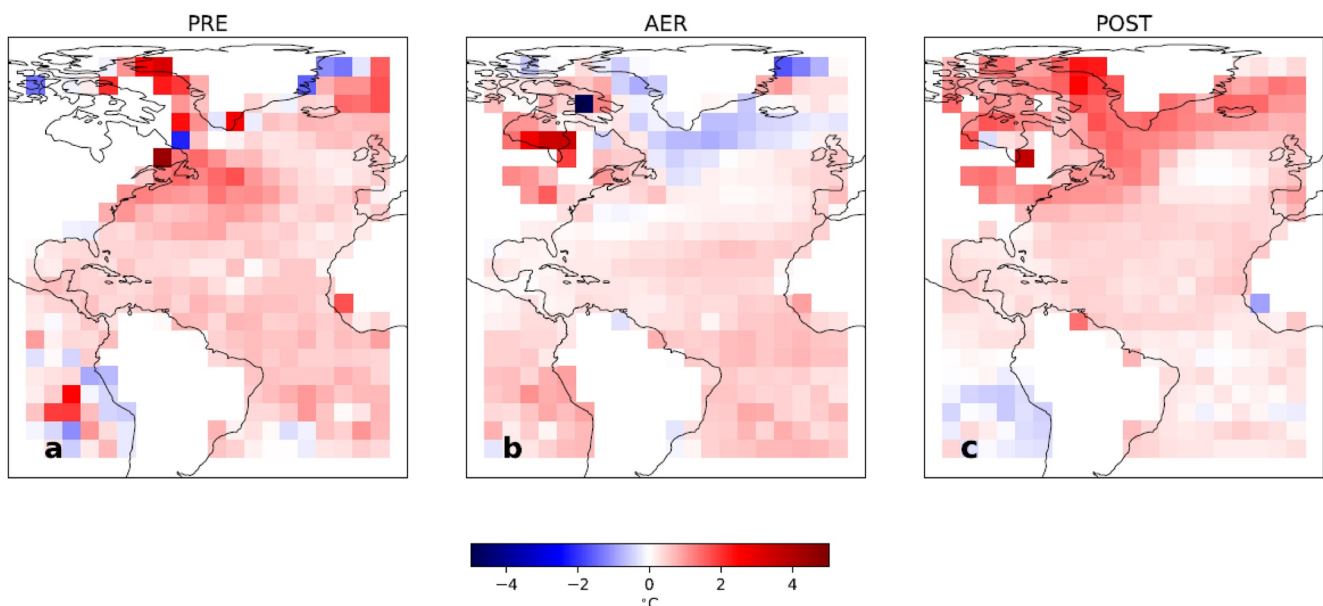


**Figure 5.** Observed sea surface temperature (SST) change during (a) PRE (1930–1950 minus 1900–1920), (b) AER (1980–2000 minus 1950–1970), and (c) POST (2010–2020 minus 1995–2005) periods, from HadSST4 data (Kennedy et al., 2019).

We also analyze an index of sub-tropical North Atlantic minus global tropical SST, shown before to correlate with Sahel rainfall changes in CMIP5 models (Giannini & Kaplan, 2019; Giannini et al., 2013). This index is also marginally correlated with precipitation sensitivity during the POST period in the CMIP6 models, with models closer to the observational SST index exhibiting slightly higher precipitation sensitivity (Figure S8 in Supporting Information S1). However, the relationship is weak. Thus, taken together, the patterns found in SST simulations are consistent with the mechanism thought to underlie the observational constraint—the ability of models to reproduce the SST response to greenhouse gas forcing in regions relevant to Sahel rainfall—but they provide only limited additional evidence for this mechanism. Further work is required to better reconcile model biases in SSTs with those in Sahel rainfall during different periods in the past, and understand their implications for future rainfall changes.

The spatial distribution of rainfall anomalies and the location of the strongest rainfall increase in the Sahel region are not exactly the same in all models (Figure S3 in Supporting Information S1), reflecting uncertainties in the dynamic response of the atmospheric circulation to global warming (Monerie et al., 2020). We allow for the possibility that models may simulate the response to GHG-induced forcing correctly but with some deviation in terms of the spatial pattern of rainfall and rainfall changes. To this end, we select for every model a rectangular region encompassing, where present, the area of maximum rainfall increase in or near the central Sahel under SSP5-8.5. In most cases, this is either identical to the common central Sahel region used so far, or offset from that region by a few degrees to the South and/or East (Figure S3 in Supporting Information S1, boxes; note that boxes are chosen congruent with the respective model grid). Constraining rainfall change in these model-specific regions using the same observational estimate as before, we obtain a stronger correlation between models' historical sensitivity and projected future change (Figure S4 in Supporting Information S1). As before, the constraint excludes models with negative and (with one exception at 2°C warming) small positive rainfall changes, while retaining many of the models with the largest projected rainfall increases. The multi-model median projection in the constrained ensemble is again higher than in the full ensemble, though the difference is somewhat smaller than when using a common central Sahel region.

While we are interested in the forced response of Sahel rainfall to GHG-induced warming, internal variability could mask this forced response to some extent on the multi-decadal timescales considered here. To test the influence of internal variability, we investigate additional ensemble members from five of the models, representing between two and ten different realizations of the same model experiment. For a given model, the estimated precipitation sensitivity to GHG-induced warming can indeed differ substantially between realizations, by as much as 0.7 mm/day per degree of global warming (Figure S5 in Supporting Information S1). However, the sign of the precipitation sensitivity is consistent across all realizations: For the four models with a positive sensitivity estimated from the primary ensemble members, all other ensemble members also yield a positive sensitivity; and vice versa for one model with a negative sensitivity. Moreover, within three of the models, precipitation sensitivity is positively correlated with projected rainfall change among ensemble members; while for the other two models, there is no visible correlation. Applying the constraint to either the multi-member subset, or the full ensemble including the additional ensemble members for the five models, both yields a higher median rainfall increase under warming than without constraint; consistent with the original single-member ensemble.

The range of equilibrium climate sensitivities (ECS) in the CMIP6 model ensemble includes higher values than that of previous CMIP ensembles (Meehl et al., 2020; Zelinka et al., 2020), and the very high ECS values in some models have been deemed unlikely (IPCC, 2021). It is therefore of interest to what extent specific regional changes in the climate system are related to ECS. Regarding Sahel rainfall change, there is no clear correspondence between ECS and our results, except that out of six models with ECS below 3°C, five have a negative precipitation sensitivity during the POST period; and all six do not reproduce North Atlantic SST change patterns during the same period well (Table S2 in Supporting Information S1). High-ECS models, in contrast, do not appear to simulate a less realistic Sahel rainfall response than models with intermediate ECS.

#### 4. Conclusions

We have presented a new method to constrain central Sahel rainfall projections in global climate models, which utilizes previous findings on the relative effects of GHG and aerosol forcing and their combination. By excluding from historical data the period with strongly increasing scattering aerosol forcing in the North Atlantic sector, we quantify the rainfall response to past GHG-induced warming only, and find very similar response coefficients for two separate periods. These estimates place a strong constraint on the CMIP6 climate model simulations, in that

only a minority of models exhibit a historical rainfall response that is consistent with these observations. That said, our analysis of multi-member simulations shows that internal variability can bias the estimated response coefficients, and we also find that many model simulations for which the response coefficient is positive but below the observational range still exhibit realistic SST change patterns. This may argue against too strict a constraint on the exact value of the precipitation sensitivity; and for the sensitivity to be positive as a minimum requirement.

Our approach is based on the premise that Sahel rainfall trends are dominated by GHG forcing during the PRE and POST periods, but by aerosol forcing during the AER period; and that the response to GHG forcing can therefore be better measured when the AER period is excluded. This does not imply that aerosol forcing is irrelevant during PRE and POST; indeed, as Figure 2a shows, aerosol precursor emissions were neither zero nor stable during these periods. However, both the levels and the rates of change of aerosol emissions were much larger during AER in the regions surrounding the North Atlantic. Other regions have seen different trends; in many Asian countries, emissions have surged in recent decades (Hoesly et al., 2018). But those emissions have little bearing on aerosol burdens over the North Atlantic, which are by and large dominated by emissions in North America and Europe, with only very small contributions from other regions (Tan et al., 2018). The Atlantic Ocean is the main external source of moisture for the West African monsoon circulation (Lélé et al., 2015), and subtropical North Atlantic SSTs in particular control moisture import into the convective regions during summer (Giannini & Kaplan, 2019). In contrast, tropical atmospheric temperatures control convective stability in the Sahel, and those could be influenced by aerosol forcing in Asia or elsewhere (Biasutti, 2019). The effect of such remote aerosol forcing on Sahel rainfall in recent years is less researched (e.g., Hirasawa et al., 2022) and, if represented differently in different models, might contribute to the spread among CMIP6 models in the POST period.

In a similar vein, the constraint discussed here should be applicable to any future scenarios in which GHG forcing dominates over aerosol forcing for North Atlantic temperature change. This is the case for the SSP5-8.5 analyzed here, which features strongly increasing GHG forcing and decreasing aerosol emissions, both globally and in the Atlantic sector. Some other SSPs assume less stringent pollution control and thus project increasing aerosol emissions in Asia, and to a lesser extent also in Southern Africa and South America. However, sulfate aerosol burdens in the North American and European regions are projected to remain at or below present levels even in the “dirty” SSP3 (Lund et al., 2019). It can therefore be expected that the condition of dominant GHG forcing will also be fulfilled in scenarios such as SSP3-7.0. On the other hand, in a situation with stabilizing GHG forcing, such as in RCP2.6 after mid-century, concurrent aerosol changes would play a larger relative role, and projections of Sahel rainfall changes under such a scenario may not be well constrained by the approach presented here.

We note that the correlation among the model ensemble between past and projected future rainfall response to GHG-induced warming is relatively weak, especially at higher warming. This can be ascribed to a small number of models that simulate substantial drying during past periods of dominant GHG forcing, while simulating substantial wetting in the future scenario; a discrepancy that may warrant further investigation. Nevertheless, our approach does not depend on a correlation because we are constraining a mechanism (rainfall response to GHG-induced warming in the absence of strong aerosol forcing) by itself; the physical connection between the constraint and the variable of interest is therefore inherent.

The constraint consistently removes models with negative or small positive projected rainfall changes from the model ensemble, while retaining some of the models with very large rainfall increases. The multi-model median rainfall change by the end of the 21st century is substantially higher in the constrained ensemble than in the full ensemble. The same is true already by the 2040s, for which the constrained multi-model mean projects nearly a 50% increase over recent rainfall levels—a large rise over a short period during which additional GHG-induced global warming is virtually unavoidable, so that this finding holds irrespective of the SSP scenario. The constraint also removes models that project a drying in the early parts of the rainy season, retaining only models with increasing monthly mean rainfall throughout the season. These findings may aid the interpretation of climate model projections, and support the expectation that in a future dominated by GHG-induced warming, the central Sahel faces a much wetter rainy season.

### Data Availability Statement

The data used in this study are publicly available through the Earth System Grid Foundation (ESGF; e.g., <https://esgf-data.dkrz.de/projects/esgf-dkrz/>) for CMIP6, and at <https://catalogue.ceda.ac.uk/uuid/89e1e34ec3554d-c98594a5732622bce9> for CRU.

### Acknowledgments

The work was supported within the European Union Horizon 2020 framework (CASCADES project). We gratefully acknowledge the CMIP6 modelling teams and the CRU for making their data available. We thank M. Büchner for help with data transfers. Open access funding enabled and organized by Projekt DEAL.

### References

- Biasutti, M. (2013). Forced Sahel rainfall trends in the CMIP5 archive. *Journal of Geophysical Research: Atmospheres*, *118*(4), 1613–1623. <https://doi.org/10.1002/jgrd.50206>
- Biasutti, M. (2019). Rainfall trends in the African Sahel: Characteristics, processes, and causes. *WIREs Climate Change*, *10*(4). <https://doi.org/10.1002/wcc.591>
- Biasutti, M., Held, I. M., Sobel, A. H., & Giannini, A. (2008). SST forcings and Sahel rainfall variability in simulations of the twentieth and twenty-first centuries. *Journal of Climate*, *21*(14), 3471–3486. <https://doi.org/10.1175/2007jcli1896.1>
- Brunner, L., Pendergrass, A. G., Lehner, F., Merrifield, A. L., Lorenz, R., & Knutti, R. (2020). Reduced global warming from CMIP6 projections when weighting models by performance and independence. *Earth System Dynamics*, *11*(4), 995–1012. <https://doi.org/10.5194/esd-11-995-2020>
- Chou, C., & Neelin, J. D. (2004). Mechanisms of global warming impacts on regional tropical precipitation. *Journal of Climate*, *17*(13), 2688–2701. [https://doi.org/10.1175/1520-0442\(2004\)017<2688:mogwio>2.0.co;2](https://doi.org/10.1175/1520-0442(2004)017<2688:mogwio>2.0.co;2)
- Eyring, V., Bony, S., Meehl, G. A., Senior, C. A., Stevens, B., Stouffer, R. J., & Taylor, K. E. (2016). Overview of the coupled model Intercomparison project phase 6 (CMIP6) experimental design and organization. *Geoscientific Model Development*, *9*(5), 1937–1958. <https://doi.org/10.5194/gmd-9-1937-2016>
- Giannini, A., Biasutti, M., Held, I. M., & Sobel, A. H. (2008). A global perspective on African climate. *Climatic Change*, *90*(4), 359–383. <https://doi.org/10.1007/s10584-008-9396-y>
- Giannini, A., & Kaplan, A. (2019). The role of aerosols and greenhouse gases in Sahel drought and recovery. *Climatic Change*, *152*(3–4), 449–466. <https://doi.org/10.1007/s10584-018-2341-9>
- Giannini, A., Salack, S., Lodoun, T., Ali, A., Gaye, A. T., & Ndiaye, O. (2013). A unifying view of climate change in the Sahel linking intra-seasonal, interannual and longer time scales. *Environmental Research Letters*, *8*(2), 024010. <https://doi.org/10.1088/1748-9326/8/2/024010>
- Guengant, J.-P. (2017). Africa's population: History, current status, and projections. In H. Groth & J. F. May (Eds.), *Africa's population: In search of a demographic dividend* (pp. 11–31). Springer International Publishing. [https://doi.org/10.1007/978-3-319-46889-1\\_2](https://doi.org/10.1007/978-3-319-46889-1_2)
- Harris, I., Osborn, T. J., Jones, P., & Lister, D. (2020). Version 4 of the CRU TS monthly high-resolution gridded multivariate climate dataset. *Scientific Data*, *7*(1), 109. <https://doi.org/10.1038/s41597-020-0453-3>
- Hawkins, E., Ortega, P., Suckling, E., Schurer, A., Hegerl, G., Jones, P., et al. (2017). Estimating changes in global temperature since the preindustrial period. *Bulletin of the American Meteorological Society*, *98*(9), 1841–1856. <https://doi.org/10.1175/bams-d-16-0007.1>
- Hirasawa, H., Kushner, P. J., Sigmond, M., Fyfe, J., & Deser, C. (2022). Evolving Sahel rainfall response to anthropogenic aerosols driven by shifting regional oceanic and emission influences. *Journal of Climate*, *35*(11), 3181–3193. <https://doi.org/10.1175/jcli-d-21-0795.1>
- Hoesly, R. M., Smith, S. J., Feng, L., Klimont, Z., Janssens-Maenhout, G., Pitkanen, T., et al. (2018). Historical (1750–2014) anthropogenic emissions of reactive gases and aerosols from the Community Emissions Data System (CEDS). *Geoscientific Model Development*, *11*(1), 369–408. <https://doi.org/10.5194/gmd-11-369-2018>
- IPCC. (2021). Summary for Policymakers. In V. Masson-Delmotte, P. Zhai, A. Pirani, S. L. Connors, C. Péan, S. Berger, et al. (Eds.), *Climate Change 2021: The Physical Science Basis. Contribution of Working Group I to the Sixth Assessment Report of the Intergovernmental Panel on Climate Change* (pp. 3–32). Cambridge University Press. <https://doi.org/10.1017/9781009157896.001>
- Kennedy, J. J., Rayner, N. A., Atkinson, C. P., & Killick, R. E. (2019). An ensemble data set of sea surface temperature change from 1850: The met office hadley centre HadSST.4.0.0.0 data set. *Journal of Geophysical Research: Atmospheres*, *124*(14), 7719–7763. <https://doi.org/10.1029/2018jd029867>
- Lélé, M. I., Leslie, L. M., & Lamb, P. J. (2015). Analysis of low-level atmospheric moisture transport Associated with the West African monsoon. *Journal of Climate*, *28*(11), 4414–4430. <https://doi.org/10.1175/jcli-d-14-00746.1>
- Lund, M. T., Myhre, G., & Samsel, B. H. (2019). Anthropogenic aerosol forcing under the shared socioeconomic pathways. *Atmospheric Chemistry and Physics*, *19*(22), 13827–13839. <https://doi.org/10.5194/acp-19-13827-2019>
- Meehl, G. A., Senior, C. A., Eyring, V., Flato, G., Lamarque, J.-F., Stouffer, R. J., et al. (2020). Context for interpreting equilibrium climate sensitivity and transient climate response from the CMIP6 Earth system models. *Science Advances*, *6*(26), eaba1981. <https://doi.org/10.1126/sciadv.aba1981>
- Monerie, P.-A., Pohl, B., & Gaetani, M. (2021). The fast response of Sahel precipitation to climate change allows effective mitigation action. *NPJ Climate and Atmospheric Science*, *4*(1), 24. <https://doi.org/10.1038/s41612-021-00179-6>
- Monerie, P.-A., Sanchez-Gomez, E., & Boé, J. (2017). On the range of future Sahel precipitation projections and the selection of a sub-sample of CMIP5 models for impact studies. *Climate Dynamics*, *48*(7–8), 2751–2770. <https://doi.org/10.1007/s00382-016-3236-y>
- Monerie, P.-A., Wainwright, C. M., Sidibe, M., & Akinsanola, A. A. (2020). Model uncertainties in climate change impacts on Sahel precipitation in ensembles of CMIP5 and CMIP6 simulations. *Climate Dynamics*, *55*(5–6), 1385–1401. <https://doi.org/10.1007/s00382-020-05332-0>
- O'Neill, B. C., Tebaldi, C., van Vuuren, D. P., Eyring, V., Friedlingstein, P., Hurtt, G., et al. (2016). The scenario model Intercomparison project (ScenarioMIP) for CMIP6. *Geoscientific Model Development*, *9*(9), 3461–3482. <https://doi.org/10.5194/gmd-9-3461-2016>
- Park, J.-Y., Bader, J., & Matei, D. (2015). Northern-hemispheric differential warming is the key to understanding the discrepancies in the projected Sahel rainfall. *Nature Communications*, *6*(1), 5985. <https://doi.org/10.1038/ncomms6985>
- Rao, S., Klimont, Z., Smith, S. J., Van Dingenen, R., Dentener, F., Bouwman, L., et al. (2017). Future air pollution in the shared socio-economic pathways. *Global Environmental Change*, *42*, 346–358. <https://doi.org/10.1016/j.gloenvcha.2016.05.012>
- Schewe, J., & Levermann, A. (2017). Non-linear intensification of Sahel rainfall as a possible dynamic response to future warming. *Earth System Dynamics*, *8*(3), 495–505. <https://doi.org/10.5194/esd-8-495-2017>
- Tan, J., Fu, J. S., Dentener, F., Sun, J., Emmons, L., Tilmes, S., et al. (2018). Source contributions to sulfur and nitrogen deposition—An HTAP II multi-model study on hemispheric transport. *Atmospheric Chemistry and Physics*, *18*(16), 12223–12240. <https://doi.org/10.5194/acp-18-12223-2018>
- Tebaldi, C., Debeire, K., Eyring, V., Fischer, E., Fyfe, J., Friedlingstein, P., et al. (2021). Climate model projections from the scenario model Intercomparison project (ScenarioMIP) of CMIP6. *Earth System Dynamics*, *12*(1), 253–293. <https://doi.org/10.5194/esd-12-253-2021>
- Tschakert, P., Sagoe, R., Ofori-Darko, G., & Codjoe, S. N. (2010). Floods in the Sahel: An analysis of anomalies, memory, and anticipatory learning. *Climatic Change*, *103*(3–4), 471–502. <https://doi.org/10.1007/s10584-009-9776-y>
- Zelinka, M. D., Myers, T. A., McCoy, D. T., Po-Chedley, S., Caldwell, P. M., Ceppi, P., et al. (2020). Causes of higher climate sensitivity in CMIP6 models. *Geophysical Research Letters*, *47*(1). <https://doi.org/10.1029/2019gl085782>
- Zhang, S., Stier, P., Dagan, G., & Wang, M. (2022). Anthropogenic aerosols modulated 20th-century Sahel rainfall variability via their impacts on North Atlantic sea surface temperature. *Geophysical Research Letters*, *49*(1). <https://doi.org/10.1029/2021gl095629>